Indoor Thermal Environment and Vertical Temperature Gradient in Large Workshop of School without air-conditioning

Saori YASUI[1], Toshio YAMANAKA[1], Kazunobu SAGARA[1], Hisashi KOTANI[1], Yoshihisa MOMOI[1], and Junya YAMADA[1]

[1] Dept. of Architectural Engineering, Osaka University, Suita 565-0871 Osaka, Japan

Abstract

The purpose of this study is to figure out the characteristics of thermal environment in a workshop at school in Japan and to propose the improvement method of the thermal environment without air-conditioning systems. In this paper, measurement results of thermal environment in the workshop and calculation results of vertical temperature gradient are shown. In the measurement results, indoor air temperature became very high in summer. Solar radiation was the main factor raising the temperature of PC roof, and large vertical temperature gradient was formed. The calculation results of zonal model shows the good agreement with the measurement results for vertical temperature gradient. Then some improvement methods of the thermal environment was investigated with the calculation model, and the investigations showed that insulating PC roof is effective method to decrease indoor air temperature.

Keywords: Large space, Workshop, Measurements, Zonal model, Case study

1. Introduction

It is important to keep students' thermal comfort by fresh air supply and heat removal in workshop of school without any air-conditioning system. In large space, it is difficult to control various factors composing indoor environment, therefore, working space often has poor thermal conditions. The target of this study is the large workshop at school, where no

air-conditioning system is installed to get out of large cost for energy consumption. The purpose of this study is to figure out the characteristics of thermal environment in the large workshop at school in Japan and to propose the improvement method of thermal environment without air-conditioning systems. Thermal measurements of existing workshop and case studies of some improvement methods with zonal model are conducted. As zonal model, Togari et al. have developed simplified prediction model of vertical temperature distribution in an atrium [1] [2] [3]. In that model, air flows along wall surfaces and air streams from outlets are considered for unsteady-state heat analysis. In this paper, the calculation method considering stack ventilation for unsteady-state is presented.

2. Thermal Measurement of Existing Workshop in a High School

2.1 Outline of Measured Building

The measurement was conducted in a workshop at high school. The plan and section of the workshop are shown in Fig.1~3. The classes of machine practical are given in this workshop. A curved heavy PC roof covers the workshop and 39 fixed skylights are on the top of the roof. The workshop wasn't installed with any air-conditioning systems, and the ventilation method is cross ventilation through side windows and mechanical ventilation with 6 axial fans on the top of outer walls (See in Fig. 2).

2.2 Method of Measurement

The measurement was carried out from 6 Sep. to 19 Sep. 2009. The all classes were hold as usual, and the windows were openable freely for teachers and students through the measurement period. Measurement items and instruments are shown in Table 1, and measurement points are shown in Fig. 1 and 3. Vertical temperature gradient and the surface temperature on the ceiling and the floor were measured at the location e (See in Fig. 1). Measurement heights at other locations were 1100mm.

2.3 Measurement Results

Measurement results on three representative days are shown in Figs.4~6. The conditions of each result are shown in Table 2. Fig.4 shows the result of Case A. The fans on the outer wall didn't operate on these three days. Fig.4 (a) shows the diurnal change of temperature and amount of solar radiation on a horizontal plane. It can be seen that indoor air temperature was much higher than outdoor and reached to 40 deg. C in the afternoon. Fig. 4 (b) shows the change of vertical temperature gradient. Large temperature gradients were formed and temperature on ceiling was over 50 deg. C. Fig.5 shows the results of Case B. In Case B, side windows must have been opened from 8:30 to 14:00 and from 18:30 to 21:00. In Fig. 5 (b), decrease of temperature due to cross ventilation was seen below 3000mm height. However,

the ceiling temperature has kept high and stagnant hot air zone exists near the ceiling. Fig. 6 shows the results of Case C. In Fig. 6 (b), the ceiling temperature doesn't rise as Case A or B, and temperature gradient wasn't formed. Figs. 4~6 indicate that the main cause of hotness in the workshop is supposed to be the ceiling heated by solar radiation and stagnant hot air near the ceiling. Thus insulation of the roof and heat removal in higher part of the workshop can be efficient method to improve the thermal environment in summer.

3. Calculation of Vertical Temperature Gradient

3.1 Description of Calculation Model

Fig.7 shows the modeling of the workshop. It consists of PC roof, indoor air, floor and ground. Actually the roof is curved, but the roof is modeled as a plane for simplification, and the walls are assumed to be insulated. Each part of the workshop is divided into a limited number of zones with only horizontal boundaries, and the temperatures are calculated using forward difference. Calculation nodes are shown in Fig. 8. The heat balance equations can be written generally for each node:

$$C\rho_j \Delta x_j \frac{\theta_{j(i)}^{n+1} - \theta_{j(i)}^{n}}{\Delta t} = \lambda_j \left(\frac{\theta_{j(i-1)}^{n} - \theta_{j(i)}^{n}}{\Delta x_j} - \frac{\theta_{j(i)}^{n} - \theta_{j(i+1)}^{n}}{\Delta x_j} \right) \quad \text{(Eq.1)}$$

At the surfaces of roof, ceiling and floor, heat transfers by convection and radiation. The heat balance equation of the top node of the roof is written as follows:

$$C\rho_p \Delta x \frac{\theta_{pc(1)}^{n+1} - \theta_{pc(1)}^{n}}{\Delta t} = h\left\{\left(\theta^n + \theta^n\right) - \theta_{pc(1)}^{n}\right\} + \lambda \left(\frac{\theta_{pc(2)}^{n} - \theta_{pc(1)}^{n}}{\Delta x_{pc}}\right) \quad \text{(Eq.2)}$$

where $\theta_e = \frac{A_s J}{h_o}$

The heat balance equations for surfaces of ceiling and floor are as follows:

$$\lambda_{pc}\left(\frac{\theta_{ceil} - \theta_{pc(nx)}}{\Delta x_{pc}/2}\right) = h_{ic}\left(\theta_{ceil} - \theta_{a(1)}\right) + \varphi_{cf} h_{ir}\left(\theta_{ceil} - \theta_{fs}\right) \quad \text{(Eq.3)}$$

$$h_{ic}\left(\theta_{a(nx)} - \theta_{fs}\right) + \varphi_{fc} h_{ir}\left(\theta_{ceil} - \theta_{fs}\right) = \lambda_f \left(\frac{\theta_{fs} - \theta_{f(1)}}{\Delta x_f/2}\right) \quad \text{(Eq.4)}$$

For calculation of air temperatures, if upper zone temperature is lower than lower zone temperature, mixing due to the buoyancy becomes active. Therefore it is possible to assume $\theta_{a(i)} \approx \theta_{a(i-1)}$ [1]. In this case, large value of λ_t (apparent thermal conductivity of indoor air, $\lambda_t = 20$ [W/mK]) is used in a calculation

program for convenience. As boundary conditions, outdoor temperature and solar radiation are given by measurement or meteorological data near the workshop and the temperature at the bottom node of ground is given 16 deg. C all day. Physical properties of each part and heat transfer coefficients are shown in Table 3, 4.

3.2 Modeling of the heat transfer by stack ventilation

If side windows and skylights are opened, reduction of indoor air temperature is expected due to stack ventilation. When the workshop is ventilated, airflow at boundary of zones must be considered. Fig.9 shows the diagram of airflow distributions. Ventilation rate is calculated with pressure difference between skylights and the center height of side windows. The pressure difference and ventilation rate are as follows:

$$\Delta P = \rho_o g H - \sum_i \rho_{a(i)} g \Delta x_a \qquad \text{(Eq.5)}$$

$$Q = C_D A \sqrt{\frac{2}{\rho} \Delta P} \qquad \text{(Eq.6)}$$

The air inflow rates entering each zone are modeled following two kinds:

(1) zones above side windows : all of Q flows into the zones

(2) zones below the top of side windows : Q from outside is equally distributed to these zones

These air flow patterns are shown in Fig. 9. Then terms of heat transfer caused by airflow are added to Eq. 1:

(1) zones above side windows

$$C\rho_{a(i)} \Delta x_a \frac{\theta_{a(i)}^{n+1} - \theta_{a(i)}^{n}}{\Delta t} = \lambda_t \frac{\theta_{a(i-1)}^{n} - \theta_{a(i)}^{n}}{\Delta x_a} - \lambda_t \frac{\theta_{a(i)}^{n} - \theta_{a(i+1)}^{n}}{\Delta x_a} + C\rho_{a(i-1)} Q\theta_{a(i-1)}^{n} - C\rho_{a(i)} Q\theta_{a(i)}^{n} \qquad \text{(Eq.7)}$$

(2) zones below the top of side windows

$$C\rho_{a(i)}\Delta x_a \frac{\theta^{n+1}_{a(i)}-\theta^{n}_{a(i)}}{\Delta t} = \lambda_t \frac{\theta^{n}_{a(i+1)}-\theta^{n}_{a(i)}}{\Delta x_a} - \lambda_t \frac{\theta^{n}_{a(i)}-\theta^{n}_{a(i-1)}}{\Delta x_a} \quad (1)$$

$$+ C\rho_o \frac{Q}{N}\theta^{n}_{o} + C\rho_{a(i+1)}\left(\frac{nx_a - i}{N}Q\right)\theta^{n}_{a(i+1)} - C_p\rho_{a(i)}\left(\frac{nx_a + 1 - i}{N}Q\right)\theta^{n}_{a(i)}$$

(Eq.8)

3.3 Calculation Cases

Calculation cases are shown in Table 5. The vertical temperature gradients were calculated for September and July. The results of Case 1(in September) were compared with measured data to validate the calculation model. As solar radiation and outdoor temperature in July is lager than September, various cases of calculation are for July (Case 2~11) in order to predict the effect of some improvement methods of thermal environment in the hottest conditions.

3.4 Calculation Results

3.4.1 Comparing with measured data

The results of calculation and measurement for Case 1 are given in Fig.10 and 11. Fig.10 shows the diurnal change of solar radiation and the air temperature. It is can be seen that the calculated ceiling and floor surface temperature showed good agreement with measurement

temperature. For the indoor air temperature, the calculation results were higher than measurement from evening to early morning on each day. It is likely that no heat loss through the walls existed because of insulating assumption, and then indoor temperature didn't decrease so much at night in calculation. In the morning, calculation and measurement air temperatures were similar relatively. Fig.11 shows the vertical temperature gradient on 7 Sep. 2009. Actually, the height of ceiling is different between calculation and measurement, but ceiling temperatures of both methods are shown at the same height for convenience. In Fig.11, calculation and measurement results were quite similar except at 18:00. Therefore this calculation model can be available to predict the vertical temperature gradient at the hottest time of day.

3.4.2 Effect of roof insulation

Fig.12 shows the vertical temperature gradient in Case 2, 6, 8 and 10. It is comparing the thermal effect of the roof insulation. All calculations are at 16:00 on 15 July. It can be seen in Fig.12 that roof insulation was able to decrease the ceiling and indoor air temperatures very much. Comparing Case 6 and Case 8, high reflective paint (As=0.2) is more efficient than polystyrene foam. If both polystyrene foam and high reflective paint were adopted, the vertical temperature gradients would be little and the temperature in occupancy area would decrease to near outdoor temperature.

3.4.3 Effect of stack ventilation

Fig.13 shows the ventilation rate in Case 3~5, and Fig.14 shows the vertical temperature gradient for Case 2~ 5. The opening areas of the skylights were varied, and in Case 2, all side windows and skylights were closed. Lager the opening area of skylight is, grater the ventilation rate is (See in Fig.13). It can be seen in Fig.14, when any small areas of skylights were opened, indoor air temperature decrease widely and the amount of decrease in air temperature didn't depend strongly on the opening area of the skylights in the range of opening area assumed in the calculation. However, ceiling surface temperature didn't decrease so much as the air temperature.

Fig.15 shows the vertical temperature gradient in Case 3, 7, 9 and 11, and Fig.16 show the comparison of ventilation rates in time series. In Case 7, 9 and 11, the workshop is ventilated and the roof is insulated or painted with high reflective paint. It can be seen in Fig.16, the ventilation rates decrease due to insulation or high reflective paint in the afternoon. However, the amounts of decrease in air temperature Case 7, 9 and 11 are larger than Case 3 (See in Fig. 15).

4. Conclusions

In the thermal measurement results in the workshop, where no air-conditioning system is installed, indoor temperature became too high and large vertical temperature gradient was formed. It is thought that the cause of hotness is the solar radiation. The authors constructed the zonal model for calculation, and the model is useful to predict the vertical temperature gradient at the hottest time of day. In the calculation results of zonal model, it was made clear that the roof insulation and stack ventilation were the efficient method to decrease indoor air temperature. Although it is true the roof insulation can reduce ventilation rate, it is not necessary to mind that. When roof insulation and heat removal in higher part of workshop are combined, indoor temperature can be decreased much and become almost equal to outdoor temperature.

Acknowledgments

The authors would like to appreciate the cooperation of relevant parties of the high school.

Nomenclature

i : node number,	h_o : outdoor total heat transfer coefficient [W/ m^{2}K],
j : material name,	h_{ic} : indoor convective heat transfer coefficient [W/ m^{2}K],
Δt : time [s],	h_{ir} : indoor radiant heat transfer coefficient [W/ m^{2}K],
Δx_j : division width of material j [m],	A_s : solar absorptance [-],
n : time step,	J : amount of solar radiation [W/m^2],
nx_j : division number of material j [-],	φ_{cf} : shape factor for floor on ceiling [-],
N: number of zones below the top of side windows, [-]	φ_{fc} : shape factor for ceiling on floor [-],
$\theta_{j(i)}$: temperature at node i of material j [deg. C],	ΔP : pressure difference between side windows and skylights [Pa],
$C\rho_j$: specific heat per volume of material j [J/m^{3}K],	ρ_o : outdoor air density [kg/m^3],
λ_j : thermal conductivity of material j [W/mK],	$\rho_{a(i)}$: indoor air density at node i [kg/m^3],
θ_o : outdoor temperature [deg. C],	g : acceleration of gravity [m/s^2],
θ_e : equivalent temperature of solar radiation [deg. C],	H : height from center of side windows to skylight [m],
θ_{ceil} : surface temperature of ceiling [deg. C],	C_D : discharge coefficient [-],
θ_{fs} : surface temperature of floor [deg. C],	A : opening area [m^2],
λ_t : apparent thermal conductivity of indoor air [W/mK],	Q : ventilation rate [m^3/s]

References

1. Togari S, Arai Y, Miura K, "*A Simplified Model for Predicting Vertical Temperature Distribution in a Large Space,*" *ASHRAE Transactions*, 1993, Part 1, pp.84～99.
2. Arai Y, Togari S, Miura K, "*Unsteady-State Thermal Analysis of a Large Space with Vertical Temperature Distribution*," *ASHRAE Transactions*, 1994, Part 2, pp.396～411.
3. Takemasa, Y, Togari, S, Arai, Y, *"Application of an Unsteady-State Model for Predicting Vertical Temperature Distribution to an Existing Atrium*," *ASHRAE Transactions*, 1996, Part 1, pp.239～247.

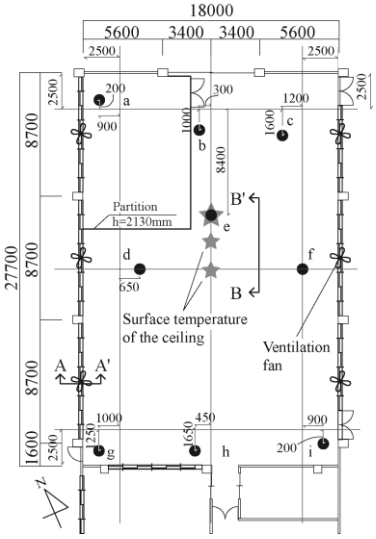

Fig. 1 Plan of the workshop

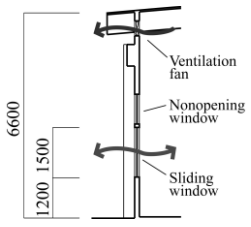

Fig. 2 Section A-A'

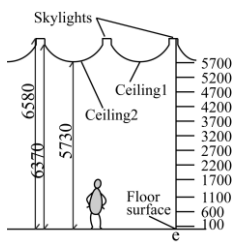

Fig. 3 Section B-B'

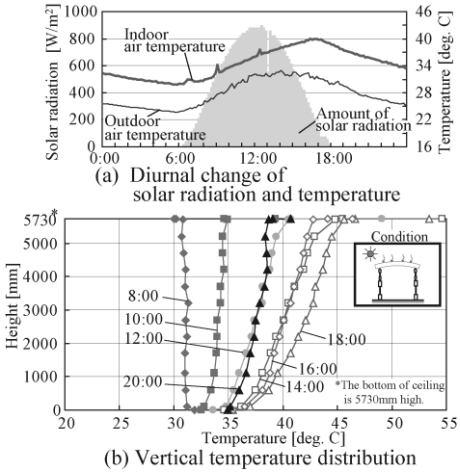

Fig. 4 Thermal measurement result (Case A)

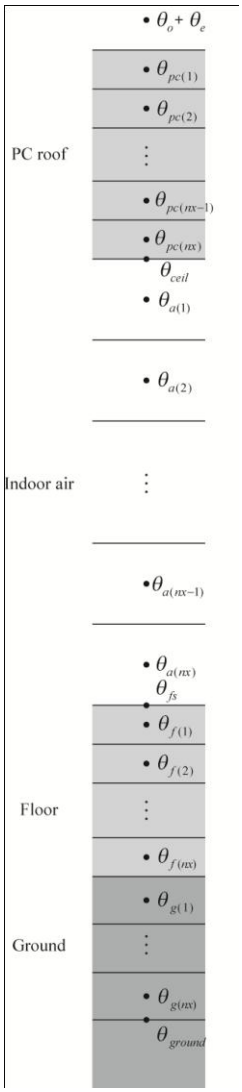

Fig. 8 Calculation nodes

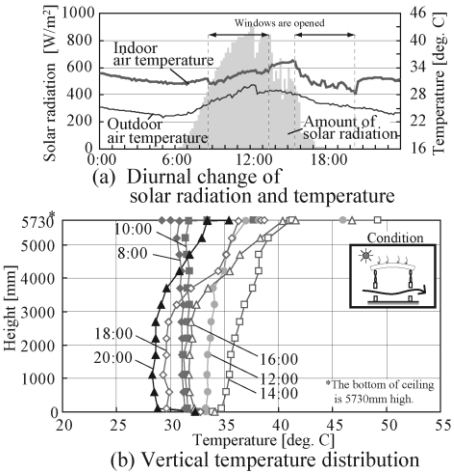

Fig. 5 Thermal measurement result (Case B)

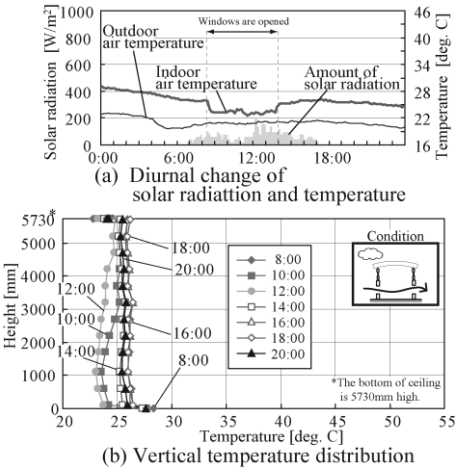

Fig. 6 Thermal measurement result (Case C)

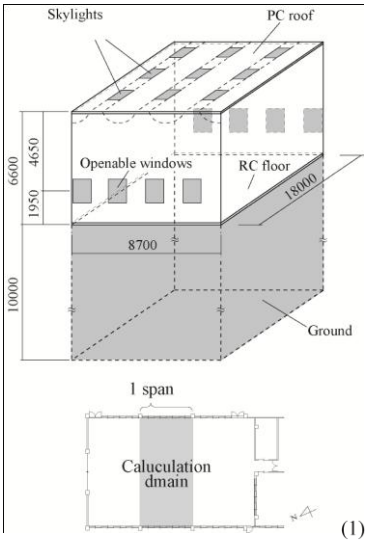

Fig. 7 Modeling of the workshop [mm]

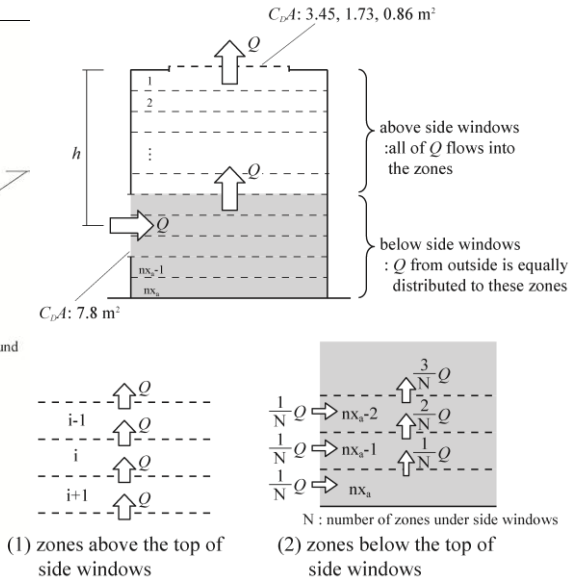

Fig. 9 Airflow by stack ventilation

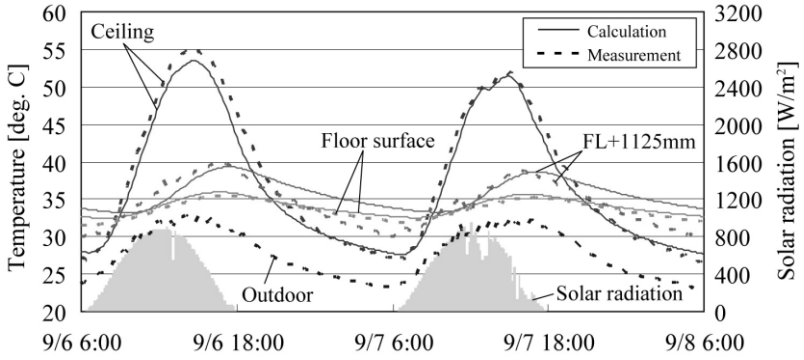

Fig. 10 Comparing calculation and measurement for diurnal change of indoor air temperature in September

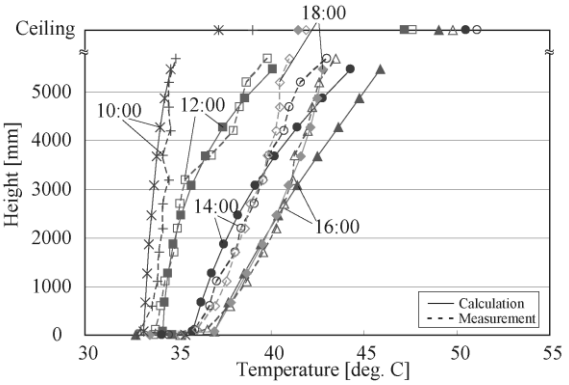

Fig. 11 Calculated and measured vertical temperature gradient in Case1(2009.9.7)

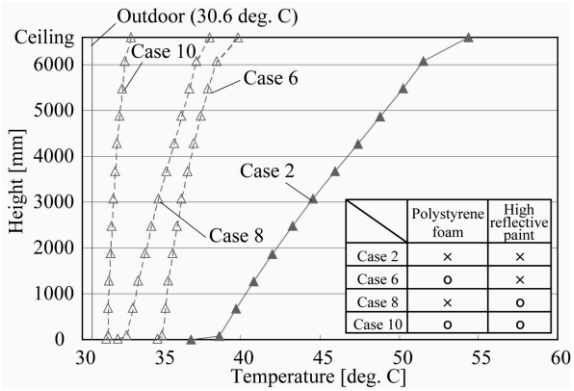

Fig. 12 Vertical temperature gradient for Case 2, 6, 8 and 10 (2009.7.15 16:00)

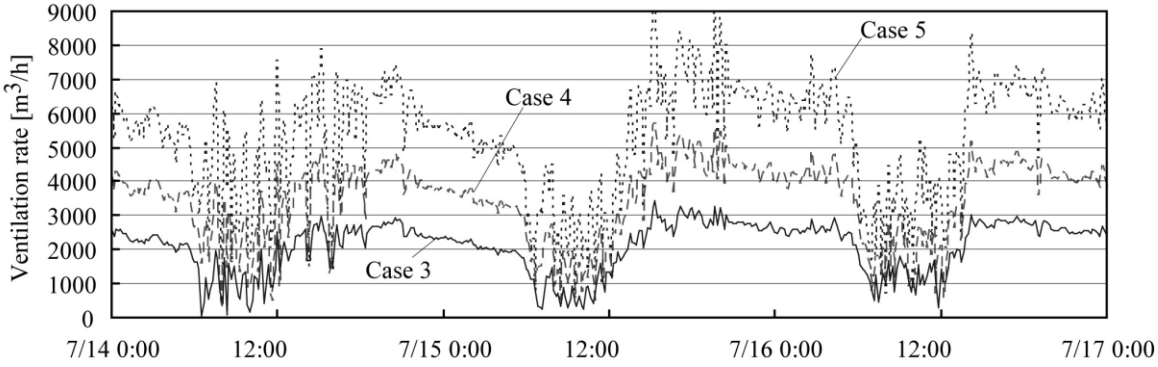

Fig. 13 Diurnal change of ventilation rate for Case 3~5

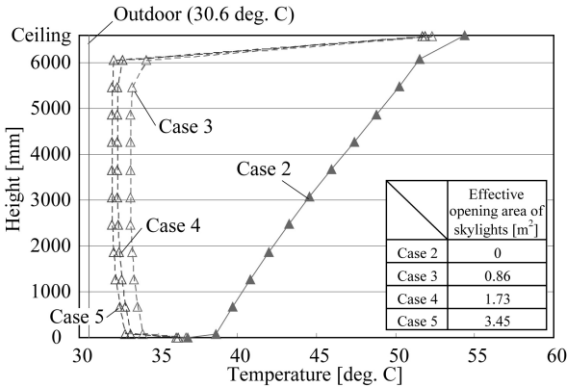

Fig. 14 Vertical temperature gradient for Case 2～5 (2009.7.15 16:00)

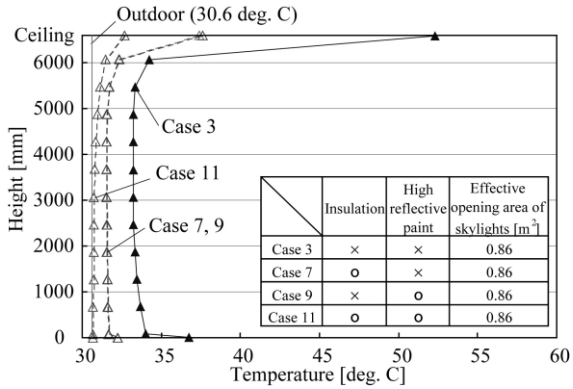

Fig. 15 Vertical temperature gradient for Case 3, 7, 9 and 11 (2009.7.15 16:00)

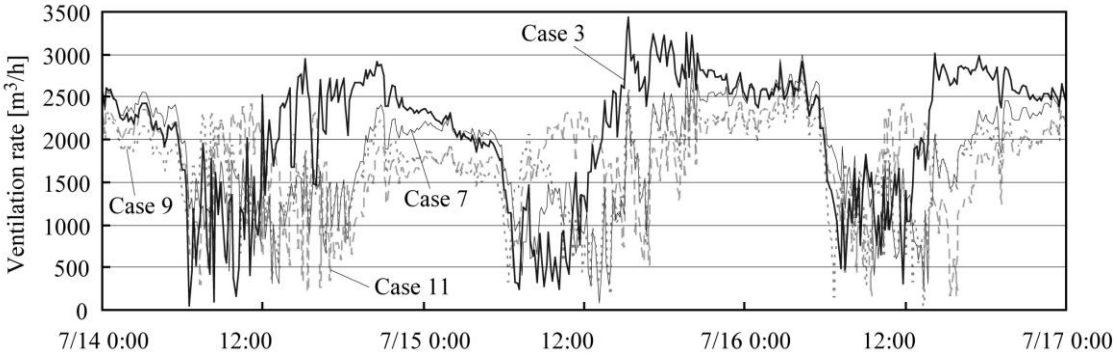

Fig. 16 Temporally change of ventilation rate for Case 3, 7, 9 and 11

Table 1 Measurement item and instrument

Measurement item	Measuring instrument	Number	Mark
Indoor air temperature, Humidity	Portable thermohygrometer T&D / RTR-53	8	●
	0.32mmϕ T type thermocouple	12	★
Surface temperature of ceiling	0.32mmϕ T type thermocouple	2	
Surface temperature of floor	0.32mmϕ T type thermocouple	1	
Outdoor air temperature, Amount of insolation, Wind direction, Wind velocity	Compact meteorological data acquisition system SEC / Weather Bucket TA-WL-2S	1	

Table 2 Condition of measurement results

	Date	Solar Radiation	Windows
Case A	2009.9.6	Large	Close
Case B	2009.9.8	Large	Open
Case C	2009.9.15	Small	Open

Table 3 Physical properties

(a) PC roof

Item		Value
l	m	0.075
λ	W/mK	1.5
ρ	kg/m^3	2400
C	J/kgK	800

(b) Indoor air

Item		Value
l	m	6.6
λ_t*	W/mK	1.16
$C\rho$	J/m^{3}K	1173.6

*λ_t : Apparent themal conductivity

(c) RC floor

Item		Value
l	m	0.15
λ	W/mK	1.4
ρ	kg/m^3	2200
C	J/kgK	880

(d) Ground

Item		Value
l	m	10
λ	W/mK	1.85
$C\rho$	J/m^{3}K	3916000

(e) Polystyrene foam

Item		Value
l	m	0.02
λ	W/mK	0.037
ρ	kg/m^3	28
C	J/kgK	1300

Table 4 Heat transfer coefficient

Item			Value	
Outdoor total heat transfer coefficient	h_o	W/m^{2}K	23	
Indoor convective heat transfer coefficient	h_{ic}	W/m^{2}K	1.13	Natural convection, heat flow : downward
			3.99	Natural convection, heat flow : upward
			2.33	Natural ventilated, heat flow : downward
			4.66	Natural ventilated, heat flow : upward
Indoor radiant heat transfer coefficient	h_{ir}	W/m^{2}K	4.97	

Table 5 Calculation Case

September

Roof : Standard Paint As=0.8		Effective Opening Area of Skylights			
		0.00 m2	0.86 m2	1.73 m2	3.45 m2
Thickness of Polystyrene Foam	0 mm	Case 1	X	X	X
	20 mm	X	X	X	X

July

Roof : Standard Paint As=0.8		Effective Opening Area of Skylights			
		0.00 m2	0.86 m2	1.73 m2	3.45 m2
Thickness of Polystyrene Foam	0mm	Case 2	Case 3	Case 4	Case 5
	20mm	Case 6	Case 7	X	X

July

Roof : High Reflective Paint As=0.2		Effective Opening Area of Skylights			
		0.00 m2	0.86 m2	1.73 m2	3.45 m2
Thickness of Polystyrene Foam	0mm	Case 8	Case 9	X	X
	20mm	Case 10	Case 11	X	X